

# Antenna Processing Optimization for a Colocated MIMO Radar

Asgeir Nysaeter  
FFI(Norwegian Defence  
Research Establishment)  
Kjeller, Norway  
Email: asgeir.nysater@ffi.no

Harald Iwe  
Radar-Sensor AS  
Oslo, Norway  
Email: Harald.Iwe@radar-sensor.as

**Abstract**—In a practical colocated MIMO radar design case, there will often not be a free choice of locations for single element antennas. Antenna parts may be available as rectangular arrays of antenna elements located on tiles, and multiple TX/RX modules may be assembled on TX/RX boards to be attached to the antenna tiles from the backside. The first part of the paper focuses on optimum attachment of transmit/receive modules to antenna tiles for a non-adaptive MIMO radar. The main lobe width and the maximum side lobe level have been minimized using genetic algorithms (GA). In the second part of the paper, transmit beamforming has been optimized using semidefinite relaxation with 4 orthogonal beams from the optimized array antenna. The antenna and processing performance using 64 active TX/RX channels have been compared to a conventional 256 elements array antenna.

## I. INTRODUCTION

The idea of Multiple-Input, Multiple Output (MIMO) radar has been known for some years [1], [2]. While non-MIMO radars emit a scaled version of the same waveform on a phased array antenna, a MIMO radar transmits linearly independent waveforms. Several potential benefits as compared to using a non-MIMO radar have been shown in the literature, such as increased number of degrees of freedom, increased virtual aperture and better possibility for a flexible beampattern design [3], [4].

Emitting linearly independent waveforms on all antenna elements gives, however, little energy transmitted per waveform, and also large processing requirements when the array size grows. By constraining the waveform independence to subarrays and by emitting a scaled version of the same waveform from each subarray, more energy is transmitted per waveform [4]. This increases the radar range and contributes to reducing the receiver processing requirements, while the increase in virtual array size may still be substantial. It is also known that better direction of arrival estimates can be achieved with higher signal-to-noise ratio (SNR) from the Cramer-Rao curves [5].

Theoretically, the TX/RX antenna elements may be moved freely on a grid in order to maximize the virtual array effect and to reduce the maximum side lobe level, but in a practical situation there may be constraints. Multiple TX/RX chains used for amplification and up-/downconversion are assembled on RF boards, and the boards must be attached to rectangular

array antenna tiles.

In the first part of the paper, an optimum array configuration is searched for conditioned on eight channel TX/RX boards and antenna tiles with 8x8 single element antennas. 64 active channels are available totally, and an array configuration is searched for minimizing the main lobe width and maximum side lobe level. The optimization is performed assuming a MIMO radar with four orthogonal beams. Four beams were used as a compromise between desired beam range, pulse length constraints, virtual array size and available processing power.

Genetic Algorithms (GA) have been used for many antenna designs [6], for sparse array design [11], and also for MIMO array optimization [10], and it has been tried for this design.

Using the resulting antenna localization and four transmit beams, the transmit beamforming power has been optimized with semidefinite relaxation [7], [8]. The aim of the present work has been to maximize both the transmit and receive antenna patterns of a non-adaptive MIMO radar.

## II. THE RECEIVE ANTENNA OPTIMIZATION PROBLEM

Fig. 1 illustrates the design restrictions. The multichannel TX/RX boards must be attached to one of the rows (columns) of an antenna tile, while the tiles can be moved along rails holding the antenna structure. New boards cannot start in one

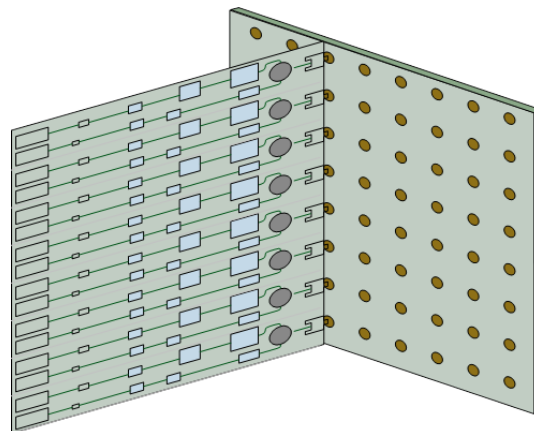


Fig. 1. Illustration of available circuit boards and antenna tiles.

of the columns to the right of the start column on the tile. Fig. 2 shows the available start positions for the circuit boards at the leftmost column on each tile (the non-greyed columns).

Setting  $N_1 = 8$  (no. of TX/RX channels per board) and  $N_2 = 4$  (no. of orthogonal beams), the MIMO array factor for a target in direction  $(\theta, \phi)$  when the array is steered at  $(\theta_0, \phi_0)$  is expressed as ( $u = \cos \theta \sin \phi, v = \sin \theta, u_0 = \cos \theta_0 \sin \phi_0, v_0 = \sin \theta_0$ )

$$F(\theta, \phi) = \sum_{i=0}^{N_1-1} \sum_{n=0}^{N_1-1} w_{i,n}^* e^{i \frac{2\pi}{\lambda} [(n_i+n)d_x(u-u_0) + m_i d_y(v-v_0)]} \cdot \sum_{m=0}^{N_2-1} v_m^* e^{i \frac{2\pi}{\lambda} [r_m(u-u_0) + t_m(v-v_0)]} \quad (1)$$

$(d_x, d_y)$  are the grid distances in the x- and y-direction,  $(n_i d_x, m_i d_y)$  are the  $(x, y)$  start positions of the boards, and  $w_{i,n}$  are the antenna receive weights.  $(r_m, t_m)$  are the phase center  $(x, y)$  positions for the four transmit beams, and  $v_m$  are complex scale factors equal to the sum of the complex transmit weights at perfect direction match. The grid is assumed nearly vertical with the z-axis pointing in the boresight direction, the x- and y-axes are in the antenna plane with the y-axis pointing upwards, and  $\theta$  and  $\phi$  are the elevation and azimuth angles respectively. Two TX/RX boards or 16 transmitters are assumed per MIMO beam.

To optimize the MIMO antenna localization, an underlying regular grid is assumed, and the antenna tiles can be moved along rails to an available grid area. The tiles cannot be moved vertically, but this is not a restriction since the TX/RX boards can be moved from an attachment position on one rail to a position on another rail. The horizontal and vertical distance between the antenna elements are assumed equal, and the distance between the top board position on a tile and the bottom board position on the tile on the rail above is equal to the distance between to adjacent horizontal or vertical antenna locations on the same tile.

The grid position has been numbered by columns from the bottom row, excluding the seven last columns to the right. Assuming 40 grid points horizontally and vertically, 1320 grid points are available as a start position for the circuit boards. The board start positions have been numbered from 1 to 1320 as an 11 bit binary number, and the eight start positions are represented as an 88 bit chromosome  $C_n = [p_1, \dots, p_{88}]$ . Comparing  $|F(\theta, \phi)|$  for the chromosomes, the fitness function is defined as

$$g(C_n) = \alpha_1 \Theta_{3dB} + \alpha_2 PSL_{dB} \quad (2)$$

where  $PSL_{dB}$  is the peak sidelobe level in dB,  $\alpha_1, \alpha_2$  are weights and  $\Theta_{3dB}$  is

$$\Theta_{3dB} = \max(\theta_B, \phi_B) \quad (3)$$

$\theta_B$  and  $\phi_B$  are the 3 dB widths of the elevation and azimuth main lobe respectively. Initially, 20 chromosomes are randomly generated. Then the 10 chromosomes with least fitness are discarded, i.e. the chromosomes with the most positive

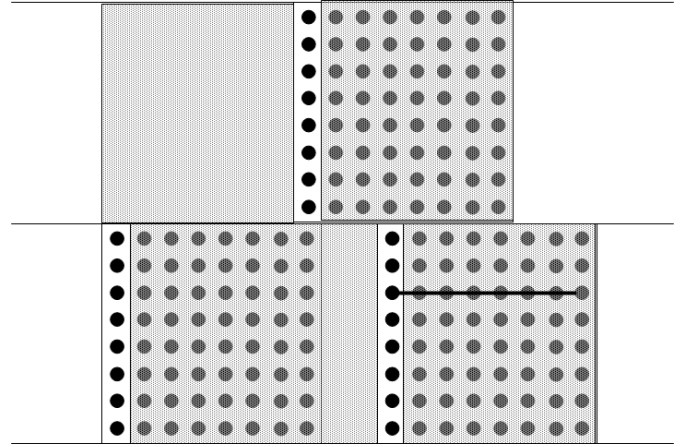


Fig. 2. Available start positions for the circuit boards are at the start column of each tile (the non-greyed columns). The tiles cannot overlap, but can otherwise be moved along the rails on the antenna grid.

fitness values. The 10 most fittest chromosomes are selected for reproduction of 10 new chromosomes. The probability for selection is given by

$$P(C_n) = \frac{|g(C_n)|}{\sum_{i=1}^{10} |g(C_i)|} \quad (4)$$

where  $C_n$  and  $C_i$  belong to the 10 most fittest chromosomes. The children are generated by two point crossover [9], a random portion (random start and random length) of the two selected parent chromosomes is exchanged to produce two new children. The mutation probability is set to 1 %, i.e. there is a 1% probability that each bit in the children chromosomes will be flipped.

### III. SEARCH RESULTS

In Fig. 3 and Fig. 4 the azimuth and elevation receive beampatterns calculated from genetic optimization of (1) are compared to the patterns of a conventional and quadratic 256 elements array antenna. The patterns are calculated with a target in direction  $(\theta, \phi) = (0, 0)$ , and  $\alpha_2$  has been given double weight compared to  $\alpha_1$ , i.e. the maximum sidelobe level is weighted more than the maximum mainlobe width. All the antenna weights are initially set to 1.

An improvement of the 3 dB main lobe width from  $14^\circ$  to  $2.8^\circ$  and  $3.4^\circ$  for the MIMO antenna can be seen from the figures. The width of the MIMO antenna is larger in azimuth than in elevation, giving a smaller main lobe in azimuth than in elevation. The maximum side lobe level for the MIMO antenna in azimuth is -21.7 dB, while it is -12.8 dB for the conventional antenna. In elevation the conventional antenna has a slightly lower maximum sidelobe level, -12.8 dB versus -12.2 dB. Obviously the main lobe width of the MIMO antenna is smaller than the conventional antenna owing to a larger antenna width both in azimuth and elevation, but the side lobe level is lower in azimuth and comparable in elevation with a fourth of active antennas.

The optimum array localization from the genetic search is

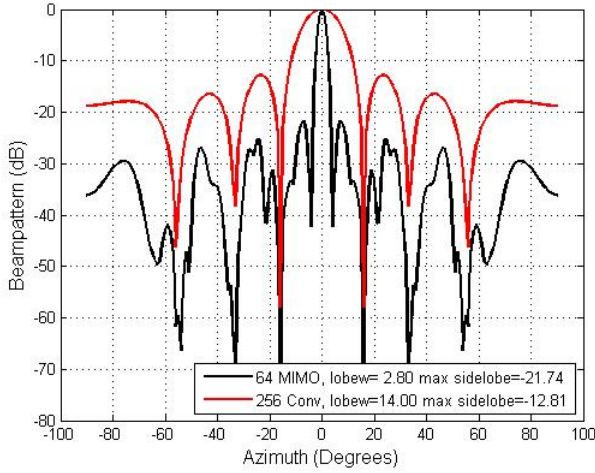


Fig. 3. The azimuth antenna pattern of a genetic optimized 64 element MIMO array compared to a 256 element conventional array.

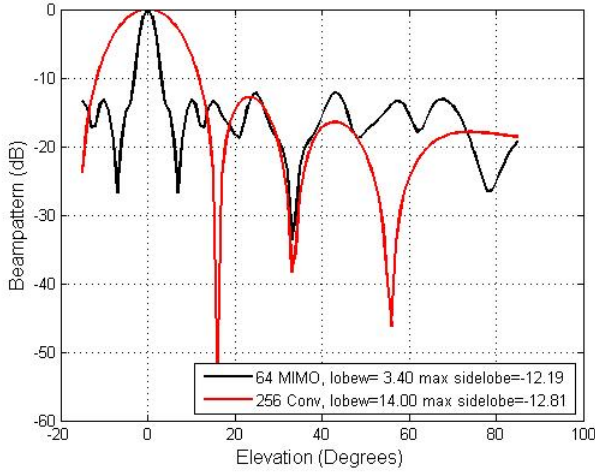


Fig. 4. The elevation antenna pattern of a genetic optimized 64 element MIMO array compared to a 256 element conventional array.

shown in Fig. 5. Eight antenna tiles are needed. The picture also shows the phase centers for the four MIMO beams, and the virtual array localization (in magenta).

#### IV. TRANSMIT BEAM OPTIMIZATION

Using the optimized antenna localization, the four orthogonal transmit beams have been optimized with regard to main- and sidelobe power in the scan direction. The signal vector from the transmit antenna is expressed as

$$\mathbf{s}_{\theta,\phi}(lT_s) = \mathbf{a}(\theta, \phi) \circ \mathbf{V}\psi(lT_s) \quad l = 0, \dots, L-1 \quad (5)$$

where  $\circ$  is the Hadamard product,  $L$  is the number of wave samples, and  $T_s$  is the sample interval.  $\mathbf{a}(\theta, \phi)$  is the transmit

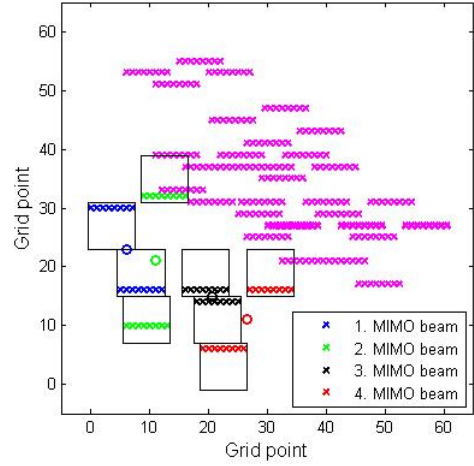


Fig. 5. Optimum antenna localization. Circles show the 4 MIMO transmit beam phase centers, and the virtual receive array is shown in magenta.

beam steering vector,

$$\mathbf{a}(\theta, \phi) = \begin{bmatrix} e^{-i\frac{2\pi}{\lambda}[n_0 d_x \sin(\phi) \cos(\theta) + m_0 d_y \sin(\theta)]} \\ \vdots \\ e^{-i\frac{2\pi}{\lambda}[(n_{N_1-1} + N_1 - 1)d_x \sin(\phi) \cos(\theta) + m_{N_1-1} d_y \sin(\theta)]} \end{bmatrix} \quad (6)$$

$\mathbf{V}$  is the  $N_1^2 \times N_2$  weight matrix

$$\mathbf{V} = \begin{bmatrix} \mathbf{v}_0 & \mathbf{0} & \mathbf{0} & \mathbf{0} \\ \mathbf{0} & \mathbf{v}_1 & \mathbf{0} & \mathbf{0} \\ \mathbf{0} & \mathbf{0} & \mathbf{v}_2 & \mathbf{0} \\ \mathbf{0} & \mathbf{0} & \mathbf{0} & \mathbf{v}_3 \end{bmatrix} \quad (7)$$

where  $\mathbf{v}_j$   $j = 0, \dots, N_2 - 1$  are  $2N_1 \times 1$  weight vectors, and  $\psi(lT_s) = [\psi_0(lT_s) \psi_1(lT_s) \psi_2(lT_s) \psi_3(lT_s)]^t$  contains the orthogonal wave functions

$$\sum_{l=0}^{L-1} \psi_k(lT_s) \psi_n^*(lT_s) = \begin{cases} E & k = n \\ 0 & k \neq n \end{cases} \quad (8)$$

The sum power from the transmit vector becomes

$$\begin{aligned} P(\theta, \phi) &= \frac{1}{L} \sum_{l=0}^{L-1} \sum_{k=0}^{N_1^2-1} \sum_{m=0}^{N_1^2-1} \mathbf{s}_{\theta,\phi}^*(lT_s)_k \mathbf{s}_{\theta,\phi}(lT_s)_m \\ &= \frac{1}{L} \sum_{l=0}^{L-1} \sum_{k=0}^{N_1^2-1} \sum_{m=0}^{N_1^2-1} a_k^*(\theta, \phi) a_m(\theta, \phi) (\mathbf{V}\psi(lT_s))_k^* (\mathbf{V}\psi(lT_s))_m \\ &= \frac{E}{L} \sum_{k=0}^{N_2-1} \mathbf{a}_k^H(\theta, \phi) \mathbf{v}_k \mathbf{v}_k^H \mathbf{a}_k(\theta, \phi) \end{aligned} \quad (9)$$

where  $H$  means conjugate transpose, and  $\mathbf{a}(\theta, \phi) = [\mathbf{a}_0^t(\theta, \phi), \dots, \mathbf{a}_{N_2-1}^t(\theta, \phi)]^t$ .

We want to optimize the transmit power to be uniform in the transmit direction, and minimum outside. To get a convex

optimization problem the expression in (9) is reformulated as a trace expression [7]

$$\begin{aligned} \min_{\mathbf{V}_k} \max_{\theta \in [\theta_1, \theta_2], \phi \in [\phi_1, \phi_2]} & \left| P_d(\theta, \phi) - \sum_{k=0}^{N_2-1} \text{Tr}[\mathbf{V}_k \mathbf{a}_k(\theta, \phi) \mathbf{a}_k^H(\theta, \phi)] \right| \\ \text{s. t. } & \mathbf{V}_{0,nn}, \dots, \mathbf{V}_{(N_2-1),nn} = \frac{1}{N_1^2} \quad n = 0, \dots, 2N_1 \quad (10) \\ & \mathbf{V}_k \geq 0 \end{aligned}$$

$\mathbf{V}_k = \mathbf{v}_k \mathbf{v}_k^H$ ,  $P_d(\theta, \phi)$  is the desired power over the main beam width  $[\theta_1, \theta_2] \times [\phi_1, \phi_2]$ , and  $\text{Tr}$  is the trace operator. The results of the optimization are shown in Fig. 6-Fig. 8 for a steering direction  $(0, 0)$ . The output power has been optimized to be uniform ( $P_d(\theta, \phi) = 1$ ) in the directions  $[0, 9] \times [-9, 9]$ . CVX has been used for the optimization [13]. The side lobe damping is better than 45 dB in azimuth, and better than 4 dB in elevation.

Since  $\mathbf{V}_k$  can be expanded as a sum of eigenvalues and eigenvectors [14],

$$\mathbf{V}_k = \sum_{n=0}^{2N_1-1} \lambda_{n,k} \mathbf{e}_{n,k} \mathbf{e}_{n,k}^H \quad (11)$$

the weight vectors  $\mathbf{v}_k$  can be calculated by approximating  $\mathbf{V}_k$  by the largest eigenvalue and eigenvector. This approximation minimizes the Frobenius norm  $\|\mathbf{V}_k - \lambda_{max,k} \mathbf{e}_{max,k} \mathbf{e}_{max,k}^H\|_F$  [14].

## V. CONCLUSION

Assuming four orthogonal transmit beams and 8-channel TX/RX boards, the location of 64 MIMO antennas was optimized with regard to main lobe width and side lobe level by genetic algorithms. With the optimum antenna configuration the weights of the transmit beams were optimized with regard to power distribution.

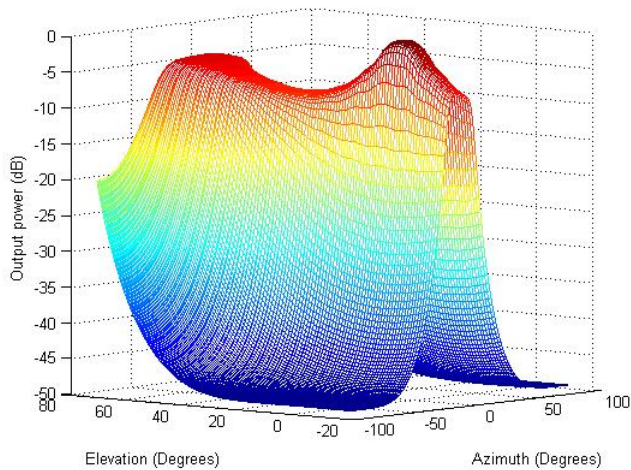


Fig. 6. Normalized antenna power pattern using 4 transmit beams in direction  $(0,0)$ .

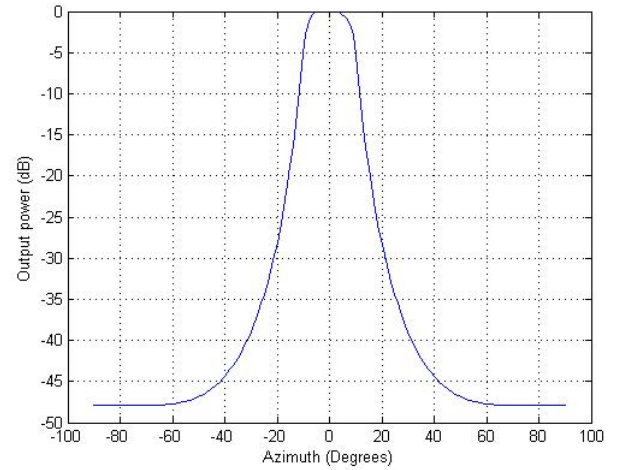


Fig. 7. Normalized antenna power pattern in azimuth using 4 transmit beams in direction  $(0,0)$ .

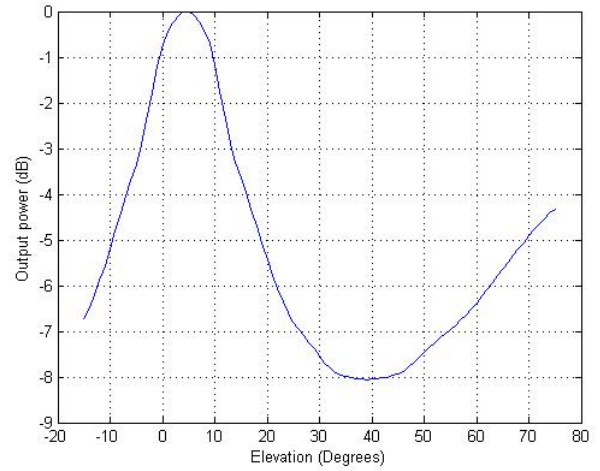


Fig. 8. Normalized antenna power pattern in elevation using 4 transmit beams in direction  $(0,0)$ .

Better elevation performance would probably be possible with more iterations. An iterative procedure would be possible by recalculating the optimum antenna localization using the calculated transmit weights, and then execute a new transmit optimization etc.. Array localization algorithms using convex cost functions based on the Cramer-Rao Lower Bound exist [12], and should be investigated in this context with regard to feasibility.

## REFERENCES

- [1] D. W. Bliss and K. W. Forsythe, "Multiple-Input Multiple-Output (MIMO) Radar and Imaging: Degrees of Freedom and Resolution," in *Proc. 37th Asilomar Conf. Signals, Systems and Computers*, Pacific Grove, CA, Nov. 2003
- [2] J. Li and P. Stoica, *MIMO Radar Signal Processing*, John Wiley & Sons, 2009.
- [3] K. W. Forsythe and D. W. Bliss, "Waveform Correlation and Optimization Issues for MIMO Radar," in *Proc. 39th Asilomar Conf. Signals, Systems and Computers*, Pacific Grove, CA, 2005.

- [4] A. Hassanien and S. A. Vorobyov, "Phased-MIMO Radar: A Tradeoff Between Phased-Array and MIMO Radars," *IEEE Transactions on Signal Processing*, June 2010.
- [5] A. Hassanien and A. S. Vorobyov, "Transmit Energy Focusing for DOA Estimation in MIMO Radar With Colocated Antennas," *IEEE Transactions on Signal Processing*, June 2011.
- [6] S. Santarelli, T.-L. Yu, D. E. Goldberg, E. Altshuler, T. O'Donnell, H. Southall, R. Mailloux, "Military antenna design using simple and competent genetic algorithms," *Mathematical and Computer Modeling*, pp. 990-1022, 2006.
- [7] Z. Q. Luo, W.-K. Ma, A. Man-Cho, Y. Ye, and S. Zhang, "Semdefinite Relaxation of Quadratic Optimization Problems," *IEEE Signal Processing Magazine*, May 2010.
- [8] A. Hassanien, M. W. Morency, A. Khabbazibasmenj, S. A. Vorobyov, J.-Y. Park, and S.-J. Kim, "Two-Dimensional Transmit Beamforming for MIMO Radar with Sparse Symmetric Arrays," in *Proc. IEEE Radar Conference*, 2013.
- [9] M. Mitchell, *An Introduction to Genetic Algorithms*, Cambridge, Massachusetts: MIT Press, 1998.
- [10] Zhaoyang Zhang, Yongbo Zhao, Jingfang Huang, "Array Optimization for MIMO Radar by Genetic Algorithms," in *2nd International Congress on Image and Signal Processing*, Oct. 2009.
- [11] Farokh Marvasti, *Nonuniform Sampling: Theory and Practice (Information Technology: Transmission, Processing and Storage)*, Springer Science+Business Media, New York, 2001.
- [12] A. A. Gorji, T. Kirubarajan, and R. Tharmarasa, "Antenna Allocation for MIMO Radars with Colocated Antennas," in *Proc. 15th International Conference on Information Fusion*, July 2012.
- [13] M. C. Grant, S. P. Boyd, *The CVX Users' Guide Release 2.1*, CVX Research Inc., 2015.
- [14] G. H. Golub, C. F. Van Loan, *Matrix Computations Third Edition*, The John Hopkins University Press, 1996.